Available online at www.sciencedirect.com
SCIENCE DIRECT®
Physica A 358 (2005) 249–262
PHYSICA A
www.elsevier.com/locate/physa

Simulation of random packing of binary sphere mixtures by mechanical contraction

Kai de Lange Kristiansen[a,b,c,*], Alan Wouterse[a], Albert Philipse[a]

[a]*Utrecht University, Van't Hoff Laboratory for Physical and Colloid Chemistry, Debye Institute, Padualaan 8, 3584 CH Utrecht, The Netherlands*
[b]*Physics Department, Institute for Energy Technology, NO-2027 Kjeller, Norway*
[c]*Department of Physics, University of Oslo, NO-0316 Oslo, Norway*

Received 14 December 2004
Available online 6 June 2005

Abstract

The mechanical contraction simulation for random dense packings is extended to binary mixture of spheres. The volume packing density as a function of sphere composition follows a characteristic triangular shape and resembles previous experiments on length scales from colloidal particles to metal shots. An excluded volume argument, which qualitatively explains trends in random packing densities of monodisperse particles, is insufficient to account for this triangular shape. The coordination number, or the average number of contacts on a sphere, shows a remarkable dip from 6 to 4 at the crossover from many small spheres to many large spheres, which has not been reported earlier. An explanation is given in terms of caging effects.

Keywords: Random packing; Coordination number; Caging; Excluded volume

1. Introduction

Random sphere packings are useful models for the microstructure of a variety of physical systems such as concentrated colloids [1], amorphous solids and glasses

*Corresponding author. Department of Physics, University of Oslo, NO-0316 Oslo, Norway. Tel.: +47 63 806077; fax: +47 63 810920.
E-mail address: k.d.l.kristiansen@fys.uio.no (K.d.L. Kristiansen).

0378-4371/$ - see front matter
doi:10.1016/j.physa.2005.03.057

[2,3], simple liquids [4] and granular matter. Apart from this modelling the random sphere packing (*rsp*)—also referred to as the Bernal packing—is of interest as a formidable challenge in itself and many studies have been devoted to the measurement [5], calculation [6] and simulation [7] of the *rsp*—density which in the large majority of cases is a sphere volume fraction close to $\phi = 0.64$. Further densification is resisted by massive structural sphere arrest which has been described in terms of jamming [8] and local caging effects [9,10]. However, still no quantitative explanation has been put forward why densification of disordered spheres grinds to a halt at or very near $\phi = 0.64$.

What has, in any case, become clear is that the very notion of a random packing (*rp*) density is not restricted to the sphere shape. It has been shown [10,11] for a large variety of randomly oriented rods and sphero-cylinders that the *rp*-density is uniquely determined by the particle aspect ratio. Quite surprisingly, in this landscape of *rp*-densities the spheres do not represent a density maximum. It was found that the *rp*-density of slightly deformed spheres is significantly above the Bernal density [10] and that the *rp*-density only starts to decrease for higher aspect ratios (the random rod packing density asymptotes to zero for increasingly thinner rods [10,11]). The near-sphere density maximum as a function of aspect ratio was qualitatively explained [10] as the result of a competition between contact numbers (which rapidly increase to arrest the rotational degrees of freedom of a non-sphere) and excluded volumes (which dominate at higher aspect ratio and drive the density down). Donev et al. [12] confirmed the existence of a near-sphere density maximum for prolate and oblate shapes and, in addition, showed that the local minimum of the Bernal *rp*-density for equal-sized spheres is actually a singularity.

Instead of increasing the *rp*-density by slight deformation of equal-sized spheres, one can also employ size-polydispersity: unequal spheres pack more densely than equal spheres. The present work is motivated by the question whether trends in random packing densities of particle mixtures can (at least qualitatively) also be understood in terms of excluded volumes and contact numbers. In other words: how strong is the similarity between the effect of particle shape and polydispersity on *rp*-densities?

It is obvious to start with the simplest example of polydispersity, namely a binary mixture of spheres, also because such mixtures have been studied experimentally in the sedimentation of colloids [13] as well as the mixing of granular particles [14]. From such experiments it is very difficult to obtain structural data such as distributions of contact numbers and radial distribution functions or to extract information on the local arrest or mobility of spheres. Recently, a simulation technique has been introduced [10] to create random packings of equal-sized spherocylinders in a wide range of aspect ratios. Here we extend the 'mechanical contraction' method [10] to binary sphere mixtures, as explained in more detail in Section 2.

2. Mechanical contraction

The aim of the mechanical contraction model [10] is to make a direct simulation of rapid densification (by sedimentation, for example) where the pressure on the particles

dominates over their thermal fluctuations. The particles are distributed in a large cell as a diluted fluid in equilibrium. The particle space is then contracted repeatedly in steps. In each step every overlap between particles is recorded and removed by relocating the particles. The directions of these particles are relocated, where the degree of overlap with contacting particles is reduced at the maximum rate. The relocation of particles is repeated until no more overlaps are detected. If the program is not able to remove the overlaps, the random dense packing of this state has been found.

The model has been useful for studying random packing of rods [10]. The algorithm can be extended to particles of different shapes and sizes and mixtures of these. Henceforth, this model should be suitable for studying the effect of particle shape and polydispersity on *rp*-densities. For a comparison to other simulation techniques, see Ref. [10].

Here, we note that the mechanical contraction method is similar to an existing Monte Carlo model given by He et al. [15]. Particles were randomly placed within a cubic box with high density. The many overlaps are relaxed by relocating the particles together with a packing space expansion. To avoid bridging, the positions of particles with coordination number less than 4 are randomly disturbed.

2.1. Details of the model

A diluted equilibrium fluid of the mixture of spheres is prepared, in a cubic cell with periodic boundary condition, using standard Monte Carlo techniques. The starting point of the cubic cell is with $4l^3$ particles, where l is an integer. In order to prevent statistical errors in our study of binary mixtures we choose the number of particles large enough so that there are at least 225 particles of the type containing fewer particles, and at least 256 particles in total. For binary mixture we used at least 2048 particles, and up to 23,328 particles.

Then we start an iterative process of reducing the particle space by reducing the volume of the cubic cell by small amounts ΔV. All of the particle positions are scaled accordingly by the factor:

$$b = \left(1 - \frac{\Delta V}{V}\right)^{1/3}. \tag{1}$$

The volume reduction starts usually with $\Delta V/V = 10^{-4}$. After a volume reduction some spheres may overlap. These spheres need to be moved apart. Let two spheres of radius r_i and r_j be in the vicinity of each other, and define $\boldsymbol{k}$ as the vector that connects the centres of these spheres. If $|\boldsymbol{k}| < D_{ij}$, where $D_{ij} = r_i + r_j$, then the two spheres overlap. The extent of the overlap is given by $\delta = D_{ij} - |\boldsymbol{k}|$. If there are C spheres which overlap with sphere i, and sphere i is moved with constant translational velocities, then the speed at which sphere i is changing its overlap with contacting sphere j may be quantified:

$$\frac{\partial \boldsymbol{k}_j}{\partial t} = \boldsymbol{k}_j \cdot \boldsymbol{a}\,, \tag{2}$$

where $\boldsymbol{a}$ is centre of mass velocity of sphere i.

The speed $\boldsymbol{s}$ for which a given particle is breaking contacts with its C overlapping particles is defined as,

$$\boldsymbol{s} = \sum_{j=1}^{C} \delta_j \frac{\partial \boldsymbol{k}_j}{\partial t} , \tag{3}$$

where the factor δ_j is included in order to bias the rate at which the particles break contact in favour of those which are overlapping most. Introduction of an additional factor for the mass of particle j is found to have no significant effect for size ratio less than 5. Therefore, we have neglected the effect of different masses of spheres of different sizes.

To obtain the direction in which to move particle i we introduce, following Ref. [10], a kinetic energy-type constraint on the velocity of particle i:

$$\boldsymbol{a}^2 = 1 . \tag{4}$$

A Lagrange multiplier is then used in Eq. (3) with the constraint Eq. (4). The directions of the velocity vector with arbitrary speed is given for each of the Cartesian coordinates $n = 1$, 2, and 3.

$$a_n = \sum_{j=1}^{C} \delta_j \frac{k_j^{(n)}}{k_j} . \tag{5}$$

Moving the particles in the direction given by Eq. (5) will reduce the degree of overlap with the C contacting particles at the maximum rate.

How far should each particle be moved? The particles need to move a small distance in order to not generate more contacts. In Ref. [10], this distance was decided to be just further than half the distance necessary to break the first contact. This means that if two and only two particles are in contact, then they are moved just far enough to break contact.

The direction and distance each particle needs to be moved is calculated and then they are all moved. This is repeated a large number of times ($\sim$5000) until there are no more overlapping pairs of particles. If the cutoff number is reached, ΔV is scaled down, typically by a factor of 0.5.

The simulation procedure is stopped when ΔV has reached a threshold value and the maximum number of attempts to remove overlaps has been performed, but failed to remove all overlaps. The densest packing for our system is taken as the packing in the previous step. A version of Verlet the neighbour list [16] is used to speed up the simulation.

3. Results and discussions

For the monodisperse case the mechanical contraction method forms a random dense packing with volume fraction $\phi_{mono} = 0.628$, consistent with previous

experimental [14] and simulation [7] studies. The same method is used to study the random dense packings of binary mixture of spheres with size ratio $\gamma = 2.6$. This γ was chosen in order to compare results directly with experiments on the rapid sedimentation of colloidal particles [13]. The experimental data are expressed in terms of the mixture of composition of the volume density of small spheres:

$$x_2 = \frac{\phi_{small}}{\phi_{total}} = \frac{N_{small} V_{small}}{N_{small} V_{small} + N_{big} V_{big}} \tag{6}$$

and in the following we will also use this variable. N_i is the number of particles of type i, V_i is the volume of one particle of type i, and ϕ_i is the volume fraction. First, we will find the packing densities as function of x_2, and try to explain qualitatively these densities by an excluded volume argument. In experiments on colloidal particles the coordination number is hard to find, while in numerical simulations this can be easily read out. We will discuss our numerical results with experiments on steel ball bearings and also relate the average number of contacts on big spheres with the parking number.

3.1. Packing densities

The random packing density clearly depends on the mixture composition. Small spheres may fill the empty space between larger spheres and thus make the structure denser. Or in another view, replacing a cluster of small spheres by a large sphere has the same effect. Fig. 1 shows a typical example of random dense packing of a binary mixture of spheres with size ratio $\gamma = 2.6$. With $x_2 = 0.528$, the volume fraction is $\phi = 0.675$ clearly above the value of the volume fraction for monodisperse spheres. The visual result from the numerical simulation (Fig. 1 (b))

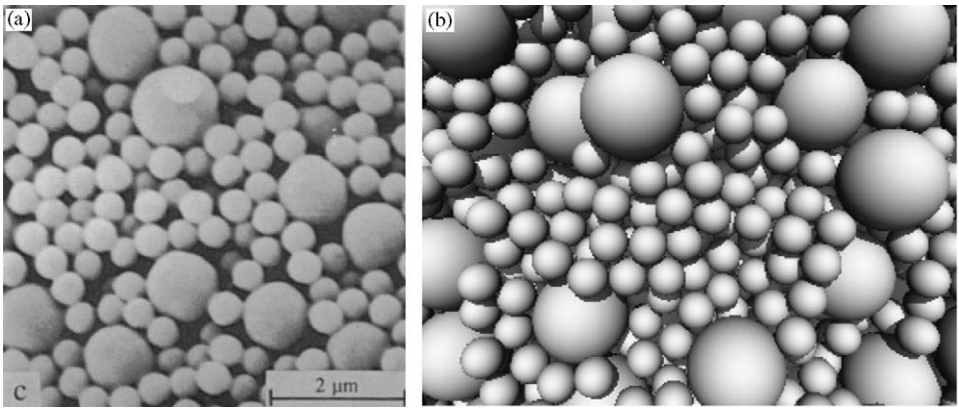

Fig. 1. Sedimentation and random dense packing of a binary mixture of spheres with size ratio of 2.6. (a) experiment from [13] with $x_2 = 0.63$ (96.8% of small spheres) and (b) the numerical simulation with the mechanical contraction model with $x_2 = 0.53$ (95% of small spheres).

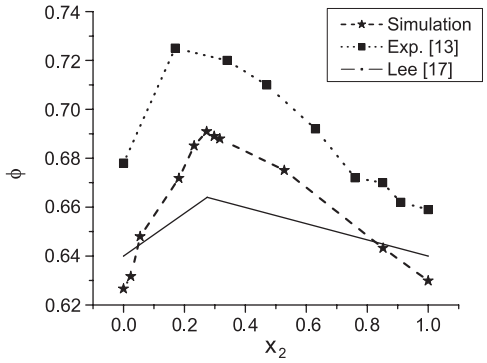

Fig. 2. The packing volume density ϕ as function of the composition of the binary mixture x_2. The square dots are from experiment on colloids [13] and the solid line is derived [17] from experiment on spherical metal shots [14]. Our simulation, star dots, resembles the characteristic triangular form found in these two experiments. Another characteristic is the maximum around $x_2 = 0.275$ and monodisperse case where ϕ should be between 0.62 and 0.64.

resembles the scanning electron microscope (SEM)-picture of colloidal particles (Fig. 1 (a)).[1]

The volume fraction ϕ as function of x_2, Fig. 2, follows a characteristic triangular shape with maximum ϕ_{max} at $x_2 = 0.275$. This behaviour is also found in experiments on binary mixture of spheres, regardless of the size ratio γ [17,18]. The high values of ϕ reported on colloidal particles may originate from ordering effect near the boundaries and also within the sample [13]. On the other hand, for metal shots ϕ are generally lower [17]. For $\gamma = 2.6$ we found $\phi_{max} = 0.691$. The simulation data reported by He et al. [15] found ϕ_{max} for x_2 equal to 0.340 and 0.400 for size ratios 2.0 and 1.5, respectively, which significantly differs from $x_2 = 0.275$ found in our results.

3.2. Contact numbers

Almost every sphere is connected to the percolating cluster of contacting spheres, as expected for a dense system of randomly packed particles. For a stable configuration of this system, a necessary condition is that each sphere needs to have at least four contacts with its neighbouring spheres. Fig. 4 shows that the average number of contacts on a sphere, the coordination number, $\langle C \rangle$ is indeed greater than 4 for all x_2. The monodisperse case has $\langle C \rangle = 5.812$, in agreement with previous studies [4,7]. In this monodisperse case it is believed that the average number of contacts is close to six contacting spheres [4]; each sphere is resting on three spheres and are supporting three other.

Let two spheres of radius r_1 and r_2 be in the vicinity of each other. The spheres are in contact if distance $|\boldsymbol{k}| < (r_1 + r_2) + \varepsilon$, where ε is a small parameter. We have used a

[1]Reprinted from [13] with permission from Elsevier.

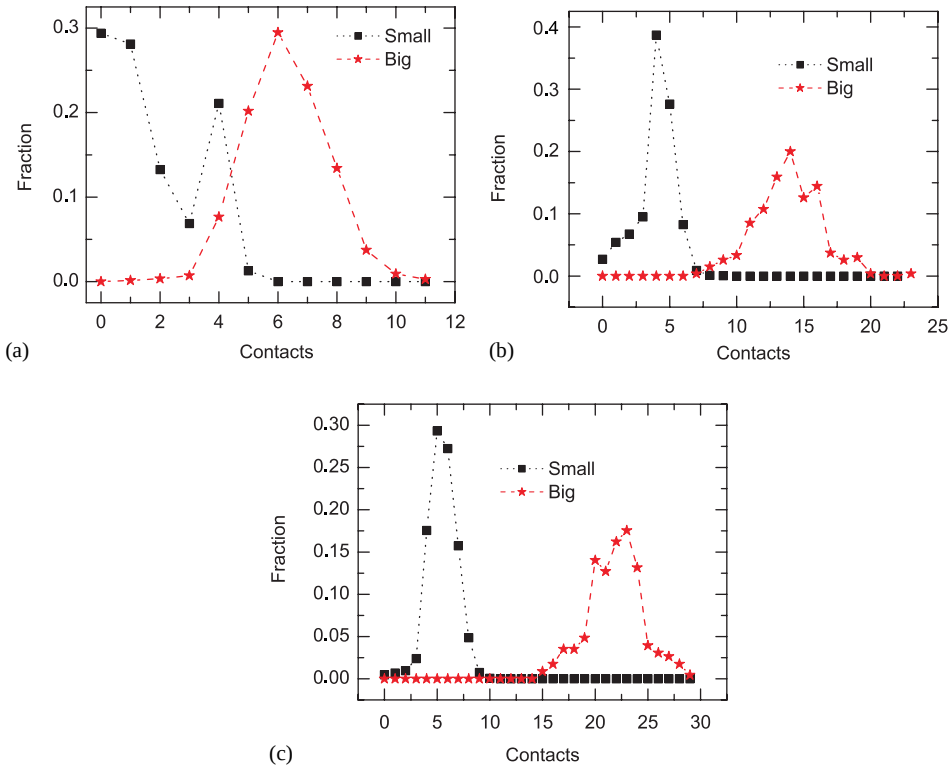

Fig. 3. The distribution of the number of contacts on small C_{small} and big spheres C_{big} for case (a) $x_2 = 0.024$, (b) $x_2 = 0.273$, and (c) $x_2 = 0.852$. In each case C_{small} has a peak around 4 contacts, while the C_{big} shift to higher values as the fraction of small spheres increases.

strict criterion $\varepsilon = 0.0005$ relative to the smallest radius. We have checked that increasing this criterion by a factor 10 does not increase the number of contacts substantially, while decreasing by a factor 2 gives no contacts.

The stabilization criterion of at least four contacts is reflected by the contacts on small spheres. For three different values of x_2, Fig. 3 shows a peak at four contacts in the distribution of the contacts on small spheres, while the average number of contacts on small spheres $\langle C_{small} \rangle$ is increasing continuously as the fraction of small particles increases until the monodisperse case where $\langle C_{small} \rangle = 5.812$ (Fig. 4). The theoretical limit of number of contacts on small spheres is 12 spheres, and in Fig. 3(c) the maximum number of contacts is 10. For low fraction of small spheres the number of contacts on big spheres is also constrained by this limit, Fig. 3(a). However, contacts on big spheres will exceed this limit because small spheres exclude less area on the surface of a large sphere than equal sized large spheres do. As the x_2 increases $\langle C_{big} \rangle$ increases, as can be seen in Fig. 5. In the limit $x_2 \to 1$, we can imagine the big spheres lying in a sea of small spheres. Since spheres are distributed randomly, this situation is similar to pack small spheres on a big sphere. The average maximum

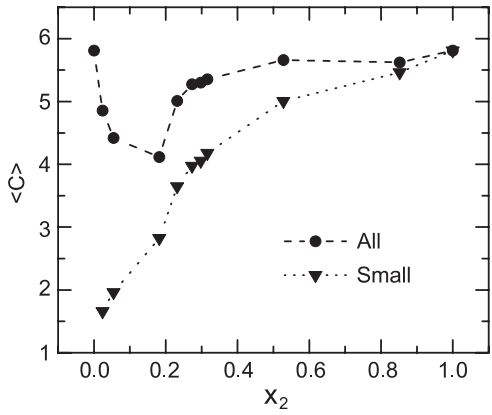

Fig. 4. The average coordination number $\langle C\rangle$ and average contact number on small spheres $\langle C_{small}\rangle$ as function of the composition of the binary mixture x_2. For the monodisperse case $\langle C_{mono}\rangle = 5.8$, as reported by other experiments and simulations. Experiments on steel ball bearings [20] yield a constant value of $\langle C\rangle = 6.2$, regardless of size ratio and composition. This is in contrast with what we observe in our model, as function of composition x_2.

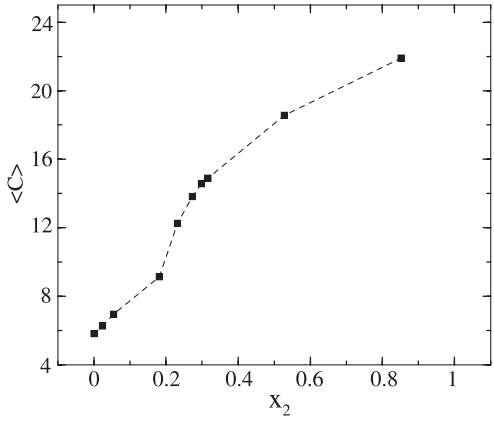

Fig. 5. Average contact number on big spheres $\langle C_{big}\rangle$ as function of composition x_2. $\langle C_{big}\rangle$ is upper bounded by the parking number of $M_p = 28.3$.

number of randomly placed small spheres on a big sphere is the so-called parking number, which is found to be [19]:

$$M_p = K_p(\gamma - 1)^2 \,, \tag{7}$$

where $K_p = 2.187$ and $\gamma = r_2/r_1$ is the size ratio between the big sphere with radius r_2 and the small sphere with radius r_1. For $\gamma = 2.6$ we have $M_p = 28.3$. We can expect that the average number of contacts on big spheres $\langle C_{big}\rangle$ is upper bounded by this

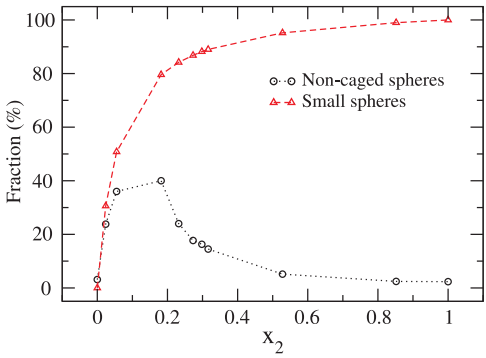

Fig. 6. The fraction of non-caged spheres as function of the composition x_2, together with the fraction of small spheres as function of the composition x_2.

parking number. The $\langle C_{big}\rangle$ in Fig. 5 near $x_2 = 1$ is somewhat lower than M_p because some small spheres will not touch.

The coordination number $\langle C\rangle$, or the average number of contacts on a sphere, is fairly constant for $0.275 < x_2 < 1.0$, with a value close to 5.8, Fig. 4. In the region $0.0 < x_2 < 0.275$, there is a remarkable dip in $\langle C\rangle$ which approaches four contact points at $x_2 = 0.182$, which is the critical value for a stable packing system. This dip is not observed in the packing experiments of steel ball bearings [20]. We note that the crossover from the low dip to the plateau of $\langle C\rangle$ occurs at $x_2 = 0.275$, which is the value with maximum close packed density. At this x_2 value it is reasonable to have a high value of $\langle C\rangle$ since we have maximum volume fraction. This also coincides with the transition from large fraction of small spheres to large fraction of big spheres, as indicated in Fig. 6.

3.3. Caging

The neglection of gravity in the model implicates that there is no preferable sedimentation direction in the system. In an ideal case, this is the situation for colloidal systems. For these systems on nanometer scale the coordination number $\langle C\rangle$ and caging effects are hard to quantify [13] and not yet explored. On larger length scales, however, as in experiments on ball bearings, preferable sedimentation direction is present. In this length scale there exist different methods to find $\langle C\rangle$ and to determine the caging effect [4,20]. The difference in packing procedure may cause different restructuring rules during the contraction and changes thus the caging procedure.

The notion of caging a sphere is closely related to the number of contacts. A sphere is caged if it is surrounded by contacting spheres such that the sphere is unable to move [21]. A surprisingly high percentage of the spheres is non-caged in the range $0 < x_2 < 0.4$, Fig. 6, and they are thus able to move. This range coincides with the transition from a low fraction of small spheres to a high fraction of small spheres,

Fig. 6. In this mixed state of spheres with two different sizes, the non-caging spheres are dominated by small spheres which are able to rattle in a jammed network of the caged spheres. The non-caging spheres have low number of contacts, and can explain the profound fall on the coordination number from above five to near four.

3.4. Excluded volume

In a hard sphere potential, a sphere cannot come closer to another sphere than the sum of their radii. The volume around a sphere restricted by this distance is called the excluded volume V_{ex}. For a polydisperse sphere system V_{ex} is a function of the radii involved. The excluded volume is then a statistical average over the number of each component, $\langle V_{ex}\rangle$. In a binary mixture of spheres:

$$\frac{1}{8}\frac{\langle V_{ex}\rangle}{\langle V_p\rangle} = \frac{f^2 + (1-f)^2\gamma^3 + \frac{1}{4}f(1-f)(1+\gamma)^3}{f + (1-f)\gamma^3}\ , \tag{8}$$

where f is the number fraction of small spheres, V_p is the volume of a sphere, and γ is the size ratio between the two sphere types.

For monodisperse spherocylinders, the orientationally average excluded volume E is proportional to the aspect ratio α for large α [22,23]. In the same limit of α, it has been shown by simulation [10] that the packing volume fraction is proportional to α, and hence E:

$$\phi \sim \frac{\langle C\rangle}{\alpha} \sim \frac{\langle C\rangle}{E}\ . \tag{9}$$

The equivalence for the volume density of a binary mixture of spheres would be

$$\phi_{ex} = \rho V_p \sim \frac{\langle C\rangle}{\langle V_{ex}\rangle/\langle V_p\rangle}\ , \tag{10}$$

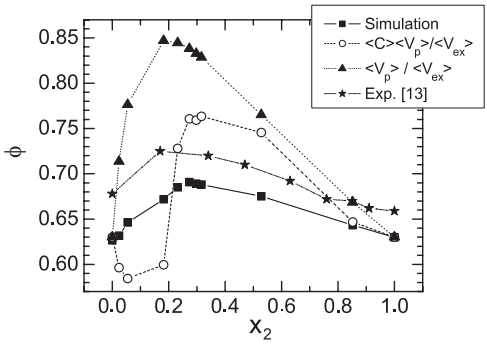

Fig. 7. The packing volume fraction ϕ of random distributed spheres together with an excluded volume argument. The square dots and the star dots display our simulation result and results from packing of colloids [13], respectively. The circular dots show the behaviour of Eq. (10), while the triangular dots show the excluded volume only.

where ρ is the density of the particles in the excluded volume argument and $\langle C\rangle$ is the coordination number, or the average number of contacts on each sphere. Fig. 7 shows that Eq. (10) is not representing ϕ as function of x_2 very well due to the strong dip in the $\langle C\rangle$ for low x_2 values. With a constant $\langle C\rangle$ as reported by [20], ϕ_{ex} gives a triangular shaped function, seen in Fig. 7, but with unphysical high value of maximum packing volume fraction.

So, we have to conclude that an excluded volume argument explains trends in packing densities of anisotropic particles much better than for asymmetric sphere mixtures. The reason is very likely that in the case of anisotropic shapes, contact correlations asymptotically vanish in the limit of very high aspect ratio [10,11], which is the justification for the scaling $\phi\sim\langle C\rangle/E$. However, when varying size ratio or composition in a sphere mixture there apparently is no such limit: contact correlations are always important and, consequently, higher-order terms must be included in Eq. (8).

4. Conclusion

We have shown that the mechanical contraction method can be extended to simulate the random dense packing of a binary mixture of spheres. In this study we have used $\gamma = 2.6$ and the volume fraction recovers the triangular behaviour as function of the sphere composition, also found in experiments on colloids and metal shots.

The coordination number $\langle C\rangle$ is important to determine the structure of the packing. In our simulation results, which may resemble rapid sedimentation of colloidal particles, we observe a remarkable dip in $\langle C\rangle$ in the region $0<x_2<0.275$. The fall in $\langle C\rangle$ from a value above five to near four at x_2 near 0.275 may be explained by the high percentage of non-caged particles and by the transition from a majority of small spheres to a majority of large spheres.

The conversion of $\langle C\rangle$ to packing densities using an excluded volume argument is much less straightforward for sphere mixtures than for anisotropic particles, very likely because contact correlations for spheres are always important, in contrast to contacts between high-aspect ratio rods. Including higher order terms in the excluded volume seems to be necessary.

Further investigations are in progress to study other size ratios and also non-spherical objects. For this purpose the mechanical contraction method seems to be very suitable.

Acknowledgements

We are grateful to Stephen Williams for providing us with his ‘mechanical contraction’ model for monodisperse particles. One of us (K.K.) thanks the Norwegian Research Council for financial support and Utrecht University for hospitality.

Appendix A. Randomness, homogeneity, and isotropy

The model was tested for its randomness, homogeneity, and isotropy for a system of particles in random close packed state. These tests are similar to the tests in Ref. [15]. The system we will present below consists of 10,976 particles where 80% of the particles are small spheres ($x_2 = 0.18$). For randomness the cell was divided into 40 slices with equal spacing and without boundary. On each slide the area density Φ_a was calculated, as seen in Fig. 8. The autocorrelation coefficient, defined as

$$P_k = \frac{\sum_{j=1}^{m-k}(s_j - \bar{s})(s_{j+k} - \bar{s})}{\sum_{j=1}^{m}(s_j - \bar{s})^2}, \tag{A.1}$$

where k is the lag which should be smaller than $m/4$, is calculated as seen in Fig. 9. If a time series is completely random, then P_k obeys $N(0, 1/m)$ normal distribution,

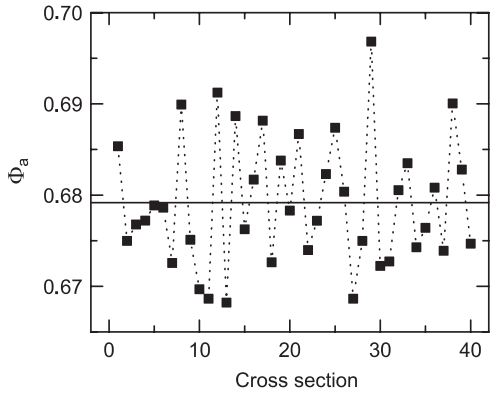

Fig. 8. The area densities Φ_a for the 40 equi-spaced slides. The mean value, indicated by the line, is 0.679.

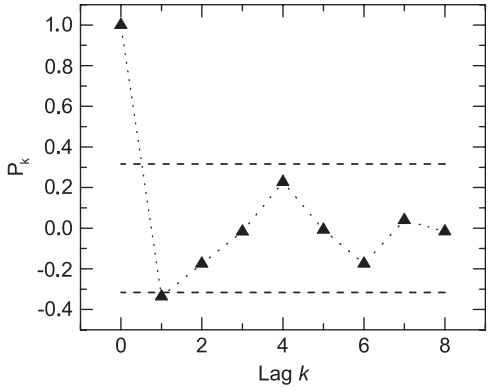

Fig. 9. The autocorrelation coefficient P_k, Eq. (A.1), of Φ_a for the first 8 lags. Nearly every point is within the 95% confidence interval.

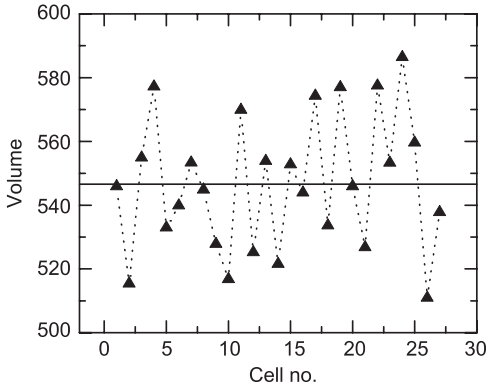

Fig. 10. The volume in each of the 27 cells the system is divided into. The mean is 546.

and over 95% of P_k is supposed to lie between $\pm 2/\sqrt{m}$. For $m = 40$ we have $2/\sqrt{m} = 0.316$. From Fig. 9 we see that most of the autocorrelation coefficients up to 8 lags is within this 95% acceptance, and supports our assumption of a random system.

For homogeneity we divide the cubic volume into 27 equal cubic subcells and calculate the volume in each subcell, Fig. 10. Thereafter, we calculate the mean and the standard deviation. For this case we found the mean volume of 546.6 ± 21.1. The standard deviation of the volume is 3.9%, and is well within accepted boundary for homogeneity.

If the system is isotropic, then the relative projections of two contact particles defined as $\Delta x_{ij} = |x_i - x_j|/(r_i + r_j)$, $\Delta y_{ij} = |y_i - y_j|/(r_i + r_j)$, and $\Delta z_{ij} = |z_i - z_j|/(r_i + r_j)$ should obey uniform distribution over (0, 1). With uniform distribution over (0, 1) the mean $\langle x \rangle = 0.5$ and standard deviation $\sigma = \sqrt{\langle x^2 \rangle - \langle x \rangle^2} = 1/2\sqrt{3} \approx 0.288675$. We found 0.499158, 0.500126, and 0.500720 as mean for projections onto x-, y-, and z-axis, respectively, with standard deviation 0.28886, 0.288917, and 0.288253, respectively. This clearly supports the assumption of an isotropic system.

References

[1] P.N. Pusey, in: J.P. Hansen, D. Levesque, J. Zinn-Justin (Eds.), Liquids, Freezing, and the Glass Transition, Elsevier, Amsterdam, 1991, p. 899.
[2] R. Zallen, The Physics of Amorphous Solids, Wiley, New York, 1983.
[3] P. Meakin, A.T. Skjeltorp, Adv. Phys. 42 (1993) 1.
[4] J.D. Bernal, J. Mason, Nature 188 (1960) 910.
[5] G.D. Scott, Nature (London) 194 (1962) 956.
[6] M. Shahinpoor (Ed.), Advances in the Mechanics and Flow of Granular Materials, vol. I, Gulf Publ. Company, Huston, 1983.
[7] B. Lubachevski, F. Stillinger, E. Pinson, J. Stat. Phys. 64 (1991) 501.
[8] S. Torquato, T.M. Truskott, P.G. Debenedetti, Phys. Rev. Lett. 84 (2000) 2064.
[9] A.P. Philipse, Colloids surfaces A 213 (2003) 167.

[10] S. Williams, A.P. Philipse, Phys. Rev. E 67 (2003) 051301.
[11] A.P. Philipse, Langmuir 12 (1996) 1127.
[12] A. Donev, I. Cisse, D. Sachs, E.A. Variano, F.H. Stillinger, R. Connelly, S. Torquato, P.M. Chaikin, Science 303 (2004) 990.
[13] D.M.E. Thies-Weesie, A.P. Philipse, J. Colloid Int. Sci. 162 (1994) 470.
[14] R.K. McGeary, J. Am. Ceram. Soc. 44 (1961) 513–522.
[15] D. He, N.N. Ekere, L. Cai, Phys. Rev. E 60 (1999) 7098–7104.
[16] M.P. Allen, D.J. Tildesley, Computer Simulation of Liquids, Oxford University Press, New York, 2002.
[17] D.J. Lee, J. Paint Technol. 42 (1970) 579.
[18] D.J. Cumberland, R.J. Crawford, The Packing of Particles, Elsevier, Amsterdam, 1987.
[19] M.L. Mansfield, L. Rakesh, D.A. Tomalia, J. Chem. Phys. 105 (1996) 3245.
[20] D. Pinson, R.P. Zou, A.B. Yu, P. Zulli, M.J. McCarthy, J. Phys. D Appl. Phys. 31 (1998) 457.
[21] E.A.J.F. Peters, M. Kollmann, Th.M.A.O.M. Barenbrug, A.P. Philipse, Phys. Rev. E 63 (2001) 021404.
[22] L. Onsager, Ann. N. Y. Acad. Sci. 51 (1949) 627.
[23] G.J. Vroege, H.N.W. Lekkerkerker, Rep. Prog. Phys. 55 (1992) 1241.